Journal of Marine Research, 58, 97–116, 2000

Generation of strong mesoscale eddies by weak ocean gyres

by Michael A. Spall[1]

ABSTRACT

The generation of strong mesoscale variability through instability of the large-scale circulation in the interior of oceanic gyres is addressed. While previous studies have shown that eddies generated from weakly sheared zonal flows are generally weak, the present results demonstrate that weakly sheared meridional flows typical of wind-forced gyres can generate very strong mesoscale variability. Meridional flows are effective at generating strong eddies because the reduced influence of the planetary vorticity gradient allows the potential energy stored in the zonal potential vorticity gradient to be converted to eddy kinetic energy. A simple scaling theory based on a balance between turbulent cascade and baroclinic energy production yields an estimate of the equilibration amplitude of the eddy kinetic energy. Nonlinear quasi-geostrophic model calculations configured in both a periodic meridional channel and a wind-driven subtropical gyre agree well with the scaling theory.

1. Introduction

It is now well recognized that the kinetic energy of the mesoscale variability in the ocean interior is much stronger than the kinetic energy of the large-scale mean circulation. Although it has been several decades since this strong mesoscale variability was first observed in the ocean (Crease, 1962; Swallow, 1971; Robinson, 1983; Stammer, 1997), there is still considerable uncertainty as to its source.

Gill *et al.* (1974) noted that the large spatial scales of the wind-driven circulation contain stores of potential energy that are several orders of magnitude larger than the kinetic energy of the mean circulation. Their results suggested that baroclinic instability of the large-scale flow might tap into this potential energy and generate mesoscale eddies of deformation radius scale that are much stronger than the mean circulation, consistent with the observed energy levels in the mesoscale band. Robinson and McWilliams (1974) also suggested baroclinic instability of the large-scale circulation as the source of the observed mesoscale variability. While they considered many environmental factors in their model, their finding that nonzonal flows are always more unstable than zonal flows on a beta-plane is particularily relevant to the present study. Because both of these studies were limited to linear instability theory, the extent to which the large-scale potential energy is available to be released into mesoscale eddies, the specific means by which this release might be achieved, and equilibration mechanisms could not be addressed.

1. Department of Physical Oceanography, Woods Hole Oceanographic Institution, Woods Hole, Massachusetts, 02543, U.S.A. ***email: mspall@whoi.edu***

Pedlosky (1975) pointed out that for weakly sheared zonal mean flows the amplitude of the perturbations is limited to be of the same order of magnitude as the mean baroclinic shear (excepting very asymmetric perturbations). This suggested that the source of the mesoscale eddies was not due to baroclinic instability of the large-scale flow but perhaps due to some other mechanism, such as radiation from distant unstable boundary currents or local atmospheric forcing.

These linear and weakly nonlinear theories were extended into the strongly nonlinear regime by Salmon (1980) and Held and Larichev (1996), hereafter HL96. The approach taken here closely follows that of HL96, in which they develop a scaling theory for the equilibration amplitude of mesoscale variability arising from baroclinic instability of a zonal mean flow on a beta-plane. Their balance at equilibration is between energy generation through baroclinic instability and energy cascade to larger scales through geostrophic turbulence. It was shown that the kinetic energy of the eddies, normalized by the mean kinetic energy, scales as $(U/\beta L_d^2)^2$, where U is the mean vertical shear, β is the meridional gradient of the planetary vorticity, and L_d is the internal deformation radius. The critical shear required for baroclinic instability occurs at $U/\beta L_d^2 = 1$. Thus, weakly sheared zonal flows are unable to generate eddy kinetic energies that are significantly larger than the mean kinetic energy, although strongly sheared flows can generate substantial eddy kinetic energies. This result is consistent with the weakly nonlinear theory of Pedlosky (1975).

In addition to providing a stabilizing influence on the mean flow, β also permits planetary waves, which provide an effective mechanism to limit the scale to which the energy can cascade (Rhines, 1975; Salmon, 1980; HL96). For the case of zonal mean flows, where the baroclinic shear is parallel to the planetary vorticity gradient, very low frequency zonal jets have been shown to develop on the large-scale mean flow (Rhines, 1975; Panetta, 1993). The meridional scale of the jets is determined by a balance between the advective velocity and the Rossby wave phase speed (Rhines, 1975).

One important difference between the mean circulation in the ocean and that of the atmosphere is that the ocean, owing to the presence of lateral boundaries, has large-scale, weakly sheared meridional flows. The idea that baroclinic instability of the large-scale wind-driven flow might be responsible for the large eddy energies observed in the ocean interiors was revisited by Spall (1994). The mean wind-driven flow in the eastern North Atlantic subtropical gyre is generally very weak and contains a component directed toward the south. Because the stabilizing influence of beta is not felt for perturbations in the zonal direction, the fastest growing perturbations for such flows are nearly zonal for almost all mean flow directions (Pedlosky, 1987; Spall, 1994). Nonlinear model calculations by Spall (1994) showed that mean shears typical of the wind-driven flow in the eastern North Atlantic could generate mesoscale eddies whose amplitude greatly exceeds that of the mean flow. This result suggests that, while the vast stores of potential energy in the large-scale flow remain inaccessible to perturbations for weakly sheared zonal mean flows, the introduction of a meridional flow component to the mean might allow zonal perturba-

tions to tap into this potential energy without feeling the effects of beta. This nonlinear model study was limited to an *f*-plane and contained no forcing so that equilibrium solutions were not possible. Meridional motions can be forced by either a wind-stress curl at the surface or by diapycnal mixing in the intermediate or deep ocean. For example, the vertical shear between the Mediterranean Water and Labrador Sea Water in the eastern North Atlantic (Spall, 1999) supports a weak meridional flow and is also susceptible to this form of baroclinic instability.

The instability and nonlinear equilibration of a nonhomogeneous meridional flow on a beta-plane has recently been studied by Dubus (1999). He also found that weak mean meridional flows could generate strong mesoscale eddies, and that equilibration involved eddy generation by baroclinic instability, Rossby wave radiation, and dissipation. Rhines (1977) also noted that weak, unforced meridional flows on a beta-plane resulting from large-scale baroclinic Rossby waves were unstable and could generate an energetic eddy field.

The generation and nonlinear equilibration of mesoscale variability by weakly sheared meridonal flows on a beta plane are the primary focus of the present study. While this work was originally motivated by the observed high eddy kinetic energies in the interior of the oceanic gyres, the approach taken here is very idealized in nature and is not intended for detailed comparison with the ocean. The primary interest is whether or not the potential energy contained in the meridional flow of the large-scale wind-driven gyres is more accessible for conversion to eddy kinetic energies than it is for purely zonal flows.

2. Scaling theory for nonlinear equilibration

A simple scaling theory for the equilibration amplitude of the eddy kinetic energy is now derived for a meridional mean flow with uniform vertical shear in a two-layer quasi-geostrophic ocean. Following HL96, it is assumed that, once the perturbations reach large amplitude, the equilibration amplitude of the eddies is determined by a balance between baroclinic eddy energy production and the cascade of energy toward larger scales in the barotropic mode. It is inherently assumed in this balance that energy is dissipated at large scales, although the specific mechanism need not be specified at this point. The results of this scaling theory, and the assumptions used in the derivation, will be tested with a series of nonlinear model calculations in the following section.

Baroclinic eddy energy production ε_p is proportional to the product of the eddy potential vorticity flux and the mean vertical shear U (Pedlosky, 1987; HL96).

$$\varepsilon_p = -U\overline{u'q'}. \tag{1}$$

For scaling purposes, it is assumed that the perturbation velocity $u' = O(V)$. The perturbation potential vorticity is proportional to a length scale l times the mean potential vorticity gradient, $q' = lQ_x$. The appropriate value for the length scale l depends on the flow configuration, as discussed further below. The potential vorticity gradient is determined by the layer thickness variation associated with the meridional mean flow,

$Q_x = U/L_d^2$, where L_d is the baroclinic deformation radius. The baroclinic energy production is now written as

$$\varepsilon_p = \frac{lU^2V}{L_d^2}. \tag{2}$$

It is assumed that the rate of energy cascade to large scales ε_c in the present forced problem scales in the same way as for two-dimensional turbulence (Rhines, 1977; HL96), where the length scale of the energy-containing eddies is given by L.

$$\varepsilon_c = V^3/L. \tag{3}$$

The normalized eddy kinetic energy at equilibration $(V/U)^2$ is then determined by equating energy production (2) with energy cascade (3).

$$(V/U)^2 = \frac{lL}{L_d^2}. \tag{4}$$

The main difference between the meridional flow configuration and the zonal flow considered by HL96 is in the determination of the appropriate length scale l. For the zonal configuration, β prohibits the eddies from traveling across the mean potential vorticity gradient (meridionally) over length scales large compared to their own scale. In this case, the perturbation potential vorticity of the eddies is limited to the potential vorticity anomaly induced over the meridional scale of the eddies, $l = L$. If the perturbations are weak, linear theory predicts that $L \approx L_d$ and (4) requires that $V/U = O(1)$, consistent with the results of HL96 and Pedlosky (1975).

Two-dimensional turbulence theory suggests that, if the perturbations are sufficiently strong, the energy-containing scales can evolve from the deformation radius toward larger scales. On an *f*-plane, this cascade appears to proceed until the eddies reach the domain size (Larichev and Held, 1995). However, Rhines (1975), Panetta (1993), and HL96 have shown that on a β-plane this cascade is halted at the length scale for which the advective velocity of the eddies matches the Rossby wave phase speed, $L = (V/\beta)^{1/2}$. At this length scale the eddies no longer are dominated by turbulent motions and, because they are influenced by variations in planetary vorticity, begin to propagate as waves. Using this scaling in (4), $l = L = (V/\beta)^{1/2}$, the result of HL96 is recovered.

$$\left(\frac{V}{U}\right)^2 = \left(\frac{L}{L_d}\right)^2 = \left(\frac{U}{\beta L_d^2}\right)^2. \tag{5}$$

For the meridional flow case, zonal motions can transport coherent water mass anomalies in the zonal direction, across mean potential vorticity contours, without being influenced by β. This means that small eddies can develop large potential vorticity anomalies because they can travel large distances across the zonal potential vorticity

gradient supplied by the mean flow. In this case, the length scale l is given by the zonal dimension of the basin (or the width of the baroclinic zone) instead of the length scale of the eddies, $l = L_x$. If it is assumed that the turbulent cascade still continues until $L = (V/\beta)^{1/2}$, the eddy kinetic energy is now

$$\left(\frac{V}{U}\right)^2 = \frac{L_x L}{L_d^2} = \left[\frac{U}{\beta L_d^2}\left(\frac{L_x}{L_d}\right)^2\right]^{2/3}. \tag{6}$$

There are several important differences between the meridional mean flow and the zonal mean flow. For zonal mean flows, the eddy kinetic energy is approximately the same as the mean kinetic energy when the mean flow is weakly sheared ($U/\beta L_d^2 = O(1)$). On the other hand, the scaling result (6) indicates that the eddy kinetic energy can be quite large even for very weakly sheared meridional flows provided that the basin is considerably wider than the internal deformation radius, which is generally the case for the basin-scale wind-driven gyres. The nonlinear model results in the following section show that large eddy energies can be generated even when $U/\beta L_d^2 < 1$. The eddy kinetic energy depends on only the ⅔ power of the criticality parameter $U/\beta L_d^2$ for meridional flows compared to the second power for the zonal flow case.

Several important assumptions have been made in deriving (6). First, it has been assumed that a source of mesoscale energy exists to provide input for the energy cascade. The growth rates for weakly sheared meridional flows, although always positive, are typically O(100 days) (Spall, 1994). Damping on time scales less than this growth rate can suppress the baroclinic instability and may inhibit the production of eddy energy. It has also been assumed that the energy cascade proceeds to the Rhines scale. It is possible that other factors, such as bottom roughness or more complex stratification, could halt this cascade at a smaller scale. In this case, the length scale L above would need to be replaced with the appropriate length scale. However, the main new point introduced here is that the production term is fundamentally different for meridional mean flows than it is for zonal mean flows.

Another important assumption is that the mean shear is uniform in space. This is clearly not the case for the large-scale oceanic wind-driven gyres. It is possible that, if the growth rates are sufficiently slow, perturbations might be advected out of the region favorable for baroclinic growth and into a more stable environment before they reach large amplitude. In this case, the length scale that determines the perturbation potential vorticity q' would be something less than the basin width L_x. This point is addressed in Section 3b (see also Dubus, 1999).

3. Nonlinear model results

The scaling theory developed in the preceeding section is now tested using a nonlinear, two-layer, quasi-geostrophic model. The model solves the quasi-geostrophic potential

vorticity equation subject to a wind-stress curl in the upper layer and dissipation in both layers.

$$\frac{\partial q_i}{\partial t} + J(\psi_i, q_i) = D_i + S_i + W_i. \tag{7}$$

The quasi-geostrophic streamfunction is ψ_i, the potential vorticity $q_i = \nabla^2\psi_i + \beta y + F_i(\psi_{3-i} - \psi_i)$, $F_i = f_0^2/g'H_i$, g' is the reduced gravity between the two layers, H_i is the layer thickness, and $i = 1, 2$ is a layer index. The β-plane approximation is used where the Coriolis parameter $f = f_0 + \beta y$. The dissipation is provided by a combination of Laplacian diffusion and a linear bottom drag.

$$D_i = A_h\nabla^4\psi_i - (i - 1)C_d\nabla^2\psi_i. \tag{8}$$

The lateral diffusivity $A_h = 10\ \mathrm{m^2\ s^{-1}}$ for all calculations. An additional dissipation is provided in the form of a sponge layer that relaxes the model potential vorticity toward q_l, where q_l is the steady flow that is in linear, inviscid potential vorticity balance with the wind-stress curl W_i.

$$S_i = -(q_i - q_l)/\gamma. \tag{9}$$

The relaxation time constant $\gamma = 180$ days within a narrow region near the western boundary, elsewhere the relaxation term is set to zero.

The model variables are discretized on a uniform finite difference grid. An enstrophy and energy conserving form of the Arakawa Jacobian is used to calculate the nonlinear terms. The potential vorticity equation is stepped forward in time using a centered leapfrog scheme with time averaging every 20 time steps to suppress computational modes. The updated streamfunction field is derived from the potential vorticity field by initially solving Helmholtz Equations for the barotropic and baroclinic modes separately and then combining to get the upper layer and lower layer streamfunctions. Details of the numerical method can be found in Beliakova (1998).

Two types of model configurations are used, a meridonal channel and an anticyclonic wind-driven subtropical gyre. The forcing and boundary conditions for each of these sets of solutions are presented in the following sections. The model is initialized with the linear, inviscid solution q_l with small perturbations of random meridional wavenumber. The amplitude of the initial perturbations is a maximum at the mid-point of the domain and decays in both the east-west and north-south directions with structure $xy(1 - x)(1 - y)$, where x is the (nondimensional) zonal distance from the edge of the sponge region and y is the (nondimensional) distance from the southern limit of the model domain. The model runs are integrated until the eddy kinetic energy reaches equilibrium. The horizontal resolution is uniform in space, and varies between 0.5 L_d and 0.75 L_d for each of the calculations.

a. Uniform meridional mean flow

The primary focus of the present study is to explore to what extent weakly sheared meridional flows might generate strong mesoscale variability. The general wind-driven subtropical gyre contains a southward component to the flow everywhere within the basin and thus will be everywhere baroclinically unstable for any nonzero vertical shear. However, the linear growth rate is strongly dependent on the direction of the mean flow (Pedlosky, 1987; Spall, 1994) and thus varies within the gyre. Before exploring the eddy generation in such a spatially variable mean state, the simpler problem of a purely meridional mean flow with uniform vertical shear is considered. The eastern and western boundaries are free-slip solid walls and the flow is periodic in the north-south direction. A uniform wind stress curl is used to force the meridional flow.

The evolution of the mesoscale eddy field is first demonstrated for a typical meridional flow configuration. The model domain in this case measures 4440 km in the zonal direction and 3840 km in the meridional direction. The sponge layer is confined to the westernmost 600 km, so that the region of fully evolving fields is 3840 km in both directions. The meridional gradient of planetary vorticity $\beta = 2 \times 10^{-13}$ cm^{-1} s^{-1} and the Coriolis parameter $f_0 = 10^{-4}$ s^{-1}. The layer thicknesses are each set to 500 m and the stratification is such that $L_d = 22.5$ km. The horizontal resolution is 15 km in both directions (296 by 256 grid points). Bottom friction is set to zero for this case. The wind stress curl is specified so that the parameter $U/\beta L_d^2 = 1.0$, where $U = 1$ cm s^{-1} is the strength of the wind-driven flow in the upper layer.

The spin-up of the mesoscale eddy field is indicated by the ratio of the kinetic energy to the initial kinetic energy as a function of time (nondimensionalized by $L_d/U = 26$ days) (Fig. 1). The kinetic energy of the initial linear, wind-driven flow is hereafter referred to as the mean kinetic energy. However, the kinetic energy of the mean flow at equilibration will generally be slightly less than this initial value because the eddy fluxes reduce the mean shear. The eddy energy is small until around time 40, when it then increases very rapidly over the next 40 time periods before leveling off. The eddy energy has essentially equilibrated by time 200 at approximately 300 times the initial kinetic energy of the wind-driven flow.

The early growth phase is characterized by zonally oriented perturbations with meridional length scales of the order of the deformation radius, consistent with linear theory and the nonlinear f-plane model results of Spall (1994). The upper layer streamfunction at time 35 is shown in Figure 2a. The perturbations initially had their maximum amplitude in the middle of the basin. Due to the beta-effect, these anomalies propagate westward as they grow so that, by the time they have reached large amplitude, the maximum perturbations are interacting with the sponge layer along the western boundary. The mean meridional flow has also advected the perturbations approximately 400 km to the south. As these perturbations grow to large amplitude, they develop strong zonal jets which themselves become unstable. The early onset of this secondary instability is just noticeable at time 35.

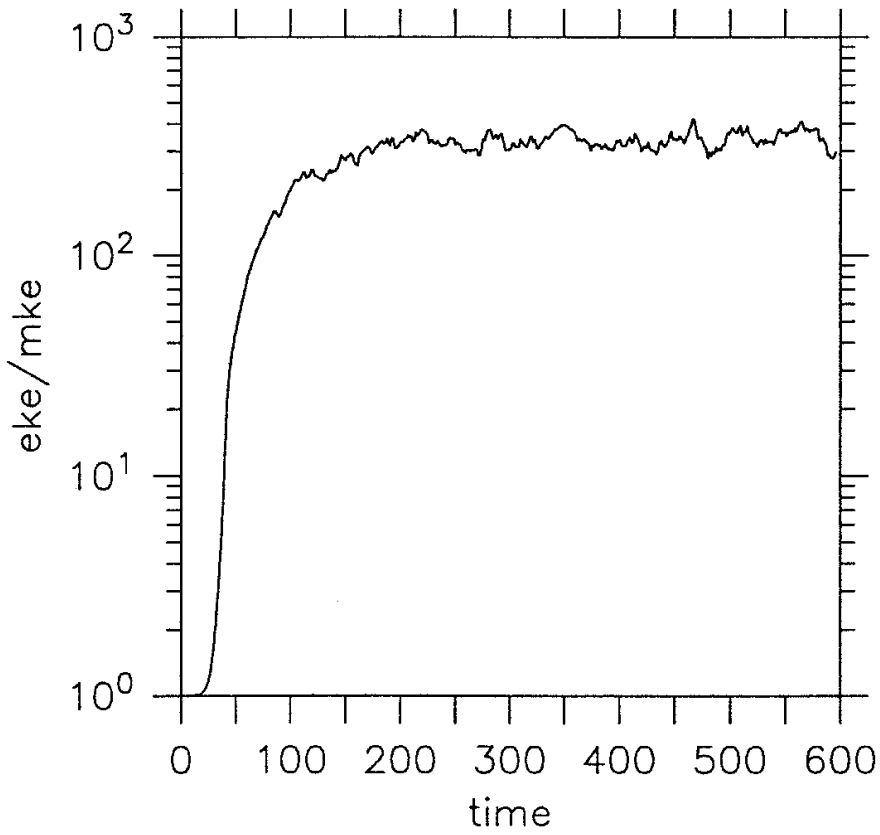

Figure 1. Ratio of eddy kinetic energy to mean kinetic energy as a function of nondimensional time for a meridional channel with $U/\beta L_d^2 = 1.0$, other parameters are defined in the text. The eddy kinetic energy is approximately 300 times the mean kinetic energy at equilibration.

After this secondary instability, the model is populated with deformation scale baroclinic eddies.

The phase of rapid growth, which begins just after the zonal jets break up into eddies, is characterized by a cascade of energy toward larger scales. The variability during the equilibrated phase is indicated by the layer 1 streamfunction at time 300 (Fig. 2b, note the change in contour interval). The domain is now populated with very strong mesoscale eddies that dominate the mean flow. While there exists variability on a range of spatial scales, the dominant energy-containing scale is considerably larger than the deformation radius (22.5 km), but still smaller than the basin-scale. The eddies are damped out within the sponge layer near the western boundary. The eddies are essentially isotropic. The introduction of eastern and western boundaries suppresses the formation of zonal jets that are commonly found in doubly periodic calculations on a β-plane (i.e., Rhines, 1975; Panetta, 1993). However, Dubus (1999) finds zonal jets to the west of a narrow region of baroclinic shear in a meridional channel calculation, so the disappearance of the zonal jets in the present case may be a result of both solid boundaries and a wide baroclinic zone.

This change in the spatial scales of the variability from the initial linear growth phase to the final equilibrated phase is further indicated by the meridional wavenumber of the zonal component of the eddy potential vorticity flux $\overline{u'q'}$ shown in Figure 3. This term is proportional to the conversion of mean potential energy to eddy kinetic energy. Early in the

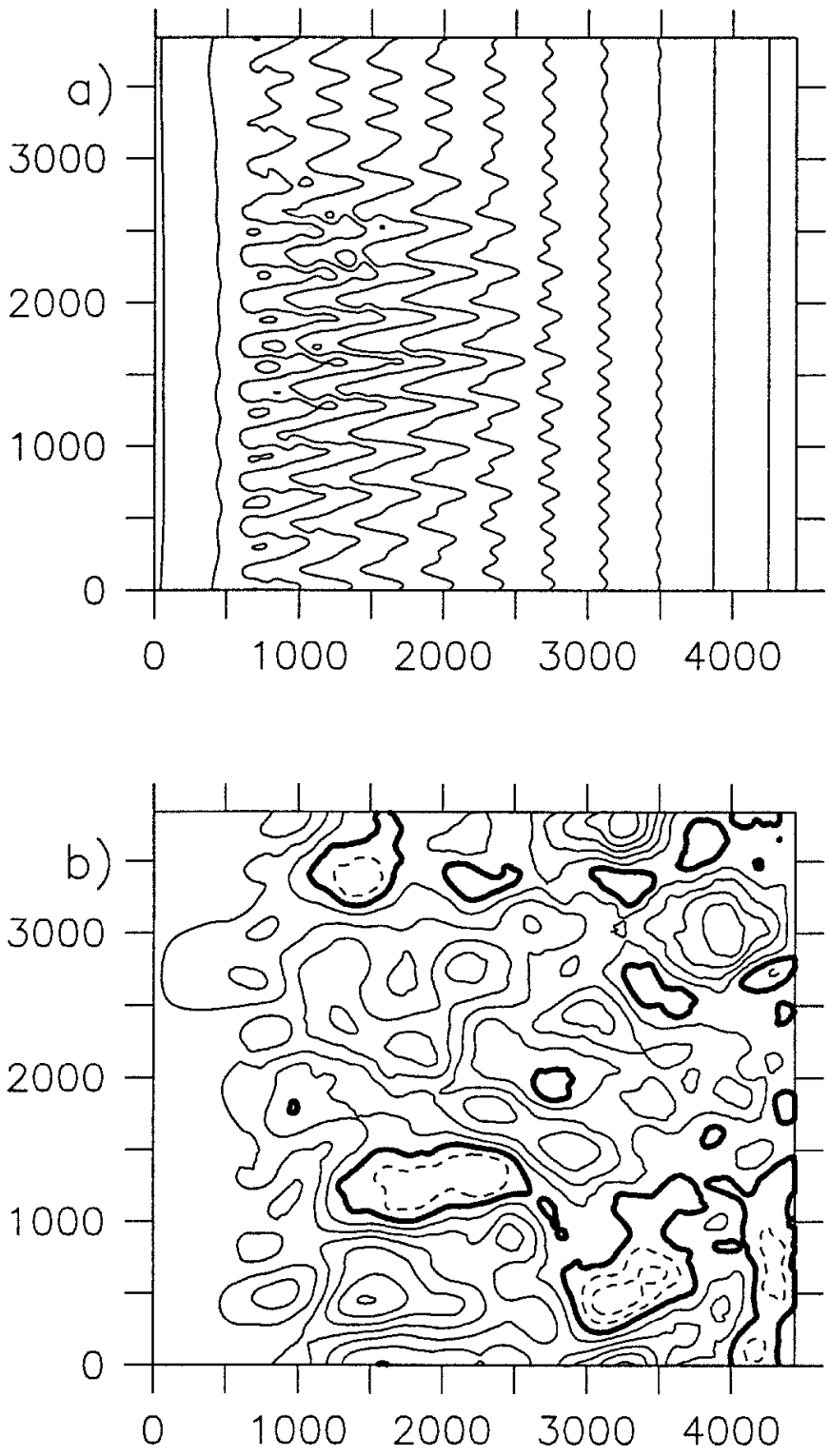

Figure 2. Layer 1 streamfunction for the meridional channel at time: (a) 35 (contour interval = 0.001); and (b) 300 (contour interval = 0.005). The early growth phase is characterized by zonal jets that themselves become unstable. The equilibrated phase is characterized by very strong, nearly homogeneous, isotropic barotropic eddies with length scales much larger than the deformation radius.

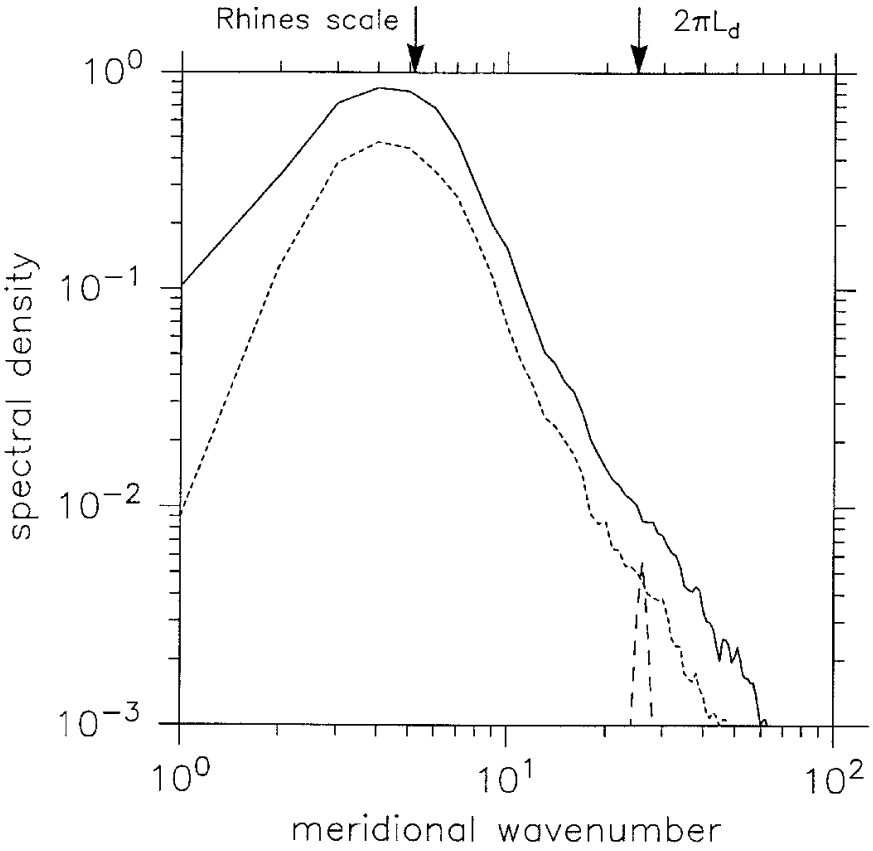

Figure 3. Spectral distribution as a function of meridional wavenumber (at $x = 3000$ km) for: the zonal eddy potential vorticity flux averaged between time 30 and 45 (dashed line); the zonal eddy potential vorticity flux averaged between times 450 and 600 (solid line) and the zonal velocity averaged between times 450 and 600 (dotted line). Early in the calculation the dominant length scales are near the deformation radius, late in the calculation the energy-containing scales, and the scales at which energy conversion is taking place, cascade to much larger scales. The Rhines scale at equilibration has wavenumber 5.2.

calculation, the zonal eddy potential vorticity flux is concentrated at meridional wavenumber 25, or a wavelength of approximately $2\pi L_d$, in general agreement with linear theory. The meridional scale of the zonal velocity is also concentrated at this wavenumber (not shown). At equilibration, the meridional scale of the zonal potential vorticity flux has shifted to wavenumbers between 3 and 6, or wavelengths between 640 km and 1280 km. The amplitude of the potential vorticity flux is also two orders of magnitude larger at equilibration than during the linear growth phase. The dominant length scale of the potential vorticity flux moves to larger scales with the dominant scale of the zonal motions. At equilibration, the Rhines scale $k_R = (\beta/V)^{1/2} \approx 5.2$, in general agreement with the dominant length scale in the model. This evolution of the energy-containing length scales, and length scales at which the energy conversion is taking place, is consistent with the cascade found for baroclinically unstable zonal flows in a doubly periodic domain by HL96.

The eddy kinetic energy is primarily in the barotropic mode at equilibration, as expected for eddies whose length scale is much greater than the internal deformation radius. The

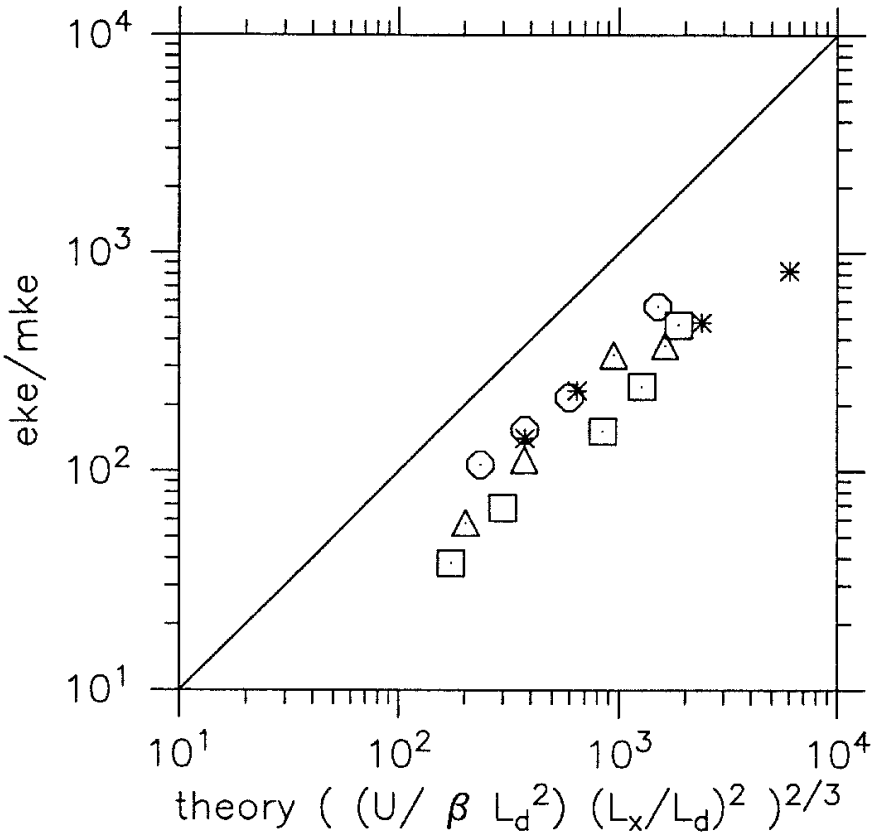

Figure 4. Comparison between the eddy kinetic energy (normalized by the mean wind-driven kinetic energy) found in the model at equilibration compared to that predicted by the scaling theory. The triangles and squares correspond to changes in the zonal extent of the domain (L_x), the circles and asterisks correspond to changes in the internal deformation radius L_d and the mean shear U. Details of the model parameters are provided in the text. The eddy kinetic energy is between 30 and nearly 1000 times greater than the mean kinetic energy. The parameter dependence predicted by the scaling estimate (6) is reasonably well reproduced by the model.

length scale of the baroclinic mode ($\psi_1 - \psi_2$) also contains significant energy at large scales, but is more white in nature with greater energy than the barotropic mode at wavenumbers greater than 20 (length scales less than about $2\pi L_d$).

The scaling theory developed in the preceeding section is now tested against a series of model calculations in the meridional channel. Four sets of calculations have been carried out in which one of the model parameters has been varied while the others are held fixed. The dependence of the equilibrated energy level diagnosed from the model calculations compares reasonably well with that predicted by the scaling theory (6), as shown in Figure 4. Although there is some scatter, the model results fall along a line that is nearly parallel to the slope predicted by the theory. The eddy kinetic energy levels range between 30 and almost 1000 times larger than the mean kinetic energy. The length scale of the energy-containing motions in each of these calculations is close to the Rhines scale assumed in the scaling theory.

The major difference between the scaling for the meridional flow and the previous result of HL96 for a zonal flow is the importance of the east-west dimension of the model

domain. Recall that it is the zonal extent of the basin (or of the baroclinic zone) that limits the amplitude of the potential vorticity anomaly that may be attained by the mesoscale eddies instead of the length scale of the eddies themselves. The importance of the channel width is clearly indicated in Figure 4. The calculations with the triangles were done with $L_y = 1500$ km, $U/\beta L_d^2 = 1.0$, and L_x was varied between 1200 km and 5760 km. The calculations indicated by the squares were carried out with $L_y = 3840$ km, $U/\beta L_d^2 = 1.5$, and L_x was varied between 1000 km and 6000 km. The eddy energy does not depend significantly on the meridional length scale (provided that it is larger than the length scale of the eddies at equilibration).

Several other parameters were varied to test the scaling estimate. Four calculations were carried out in which the basin size $L_x = 3840$ km and $U/\beta L_d^2 = 1.0$ were held fixed and L_d was set to 15.9 km, 31.8 km, 44.9 km, and 63.5 km (circles on Fig. 4). Another set of calculations was carried out in which the basin size and the ratio $U/\beta = 5 \times 10^8$ m^2 were held fixed and the deformation radius was set to 11.2 km, 15.9 km, 25.9 km, and 31.8 km ($U/\beta L_d^2 = 0.75, 1.0, 4.0\ 8.0$, asterisks). While there are of course many other possible combinations to test scaling (6), these calculations explore a reasonable range of parameter space in terms of both eddy energy levels and physical and geometric quantities. In each case, the energy level varies consistent with the scaling theory.

The scaling theory does not depend explicity on the form of dissipation, although it is assumed that energy is dissipated at large scales. In the above results, dissipation is provided by the sponge layer near the western boundary ($C_d = 0$). Potential energy is input through the wind stress at large scales. The eddy potential vorticity flux converts this large-scale potential energy to kinetic energy on the eddy length scale (which is a function of time). At equilibration, the eddies are of sufficiently large scale that energy propagates westward in the form of barotropic Rossby waves. The energy is then dissipated in the sponge layer near the western boundary.

Bottom drag, as used by HL96, is also a likely candidate to remove energy at scales larger than the deformation radius because motion on these scales is mostly barotropic. The calculations shown in Figure 4 were repeated with a linear bottom drag of strength $C_d = 0.08\ U/L_d$. Although the equilibration energies are systematically lower than without bottom drag, the results in Figure 5 indicate that the scaling (6) still applies reasonably well to the case with finite bottom drag. Calculations with both $C_d = 0$ and no sponge layer do not equilibrate within several hundred eddy turnaround times.

b. Subtropical gyre

The results of the meridional channel configuration indicate that weakly sheared meridional flows can generate eddy variability that is much stronger than the mean flow. It is not clear, however, that the same level of eddy variability could be generated by a mean flow that is not purely meridional over the entire model domain, such as would be expected for a wind-driven subtropical gyre. As the flow becomes more zonal, the mean potential vorticity gradient is aligned more parallel to the planetary vorticity gradient and the ability

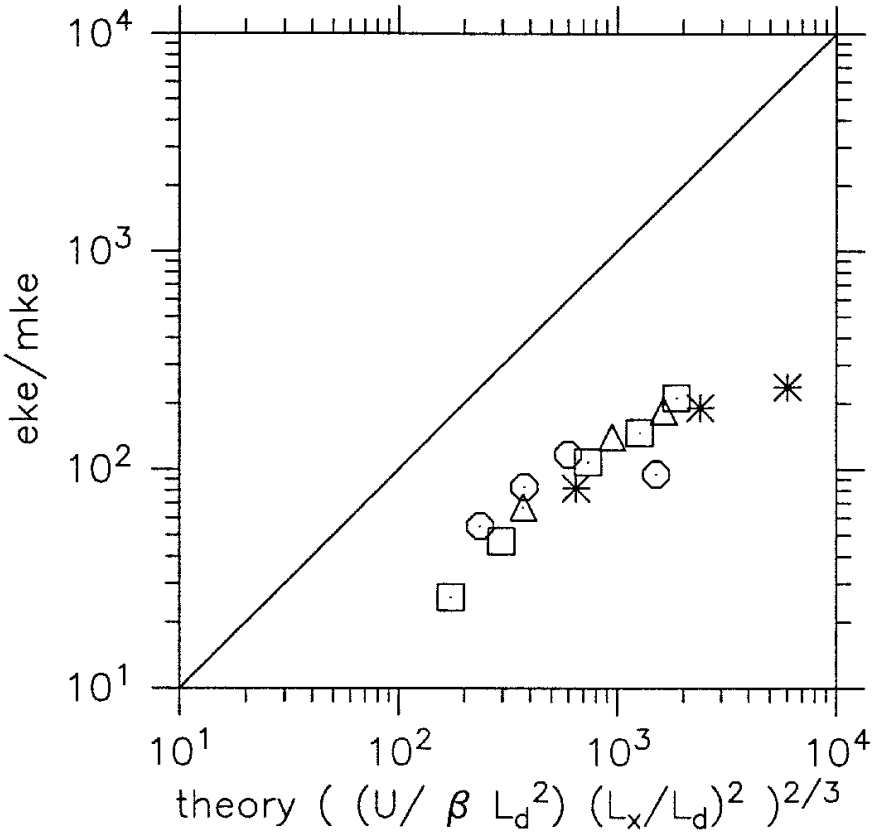

Figure 5. As in Figure 4 except with bottom drag $C_d = 0.08U/L_d$.

of perturbations to convert the potential energy of the mean flow into eddy kinetic energy is suppressed (Pedlosky, 1987; Spall, 1994). In addition, most previous studies of turbulence have been in periodic domains that allow turbulence to cascade uninhibited by lateral boundaries. The scaling theory is now tested for a nonhomogeneous mean flow generated by an anticyclonic wind stress curl.

Westward intensification of an anticyclonic wind-driven flow in a closed basin gives rise to a strong northward-flowing western boundary current. Depending on the distribution of the wind stress curl and degree of nonlinearity, such boundary currents can become unstable. Although much of the resulting variability would be confined to the immediate region of the meandering jet, some may propagate from the region of strong shear into the weakly sheared interior either in the form of coherent vortices or as radiated waves. It is unknown how much of the observed mesoscale variability in the open ocean is a result of energy radiated away from such strong frontal regions and how much might be generated by instability of the large-scale interior flow (the subject of interest here). In order to isolate the interior source from the strong boundary current source, I have configured the domain as a regional model of the interior wind-driven flow.

The subtropical gyre configuration has free slip solid walls on the southern, eastern, and northern boundaries and an open boundary condition on the western boundary. The streamfunction on the western boundary is specified to be the steady, linear inviscid solution which balances the wind-stress curl, assuming no flow through the eastern

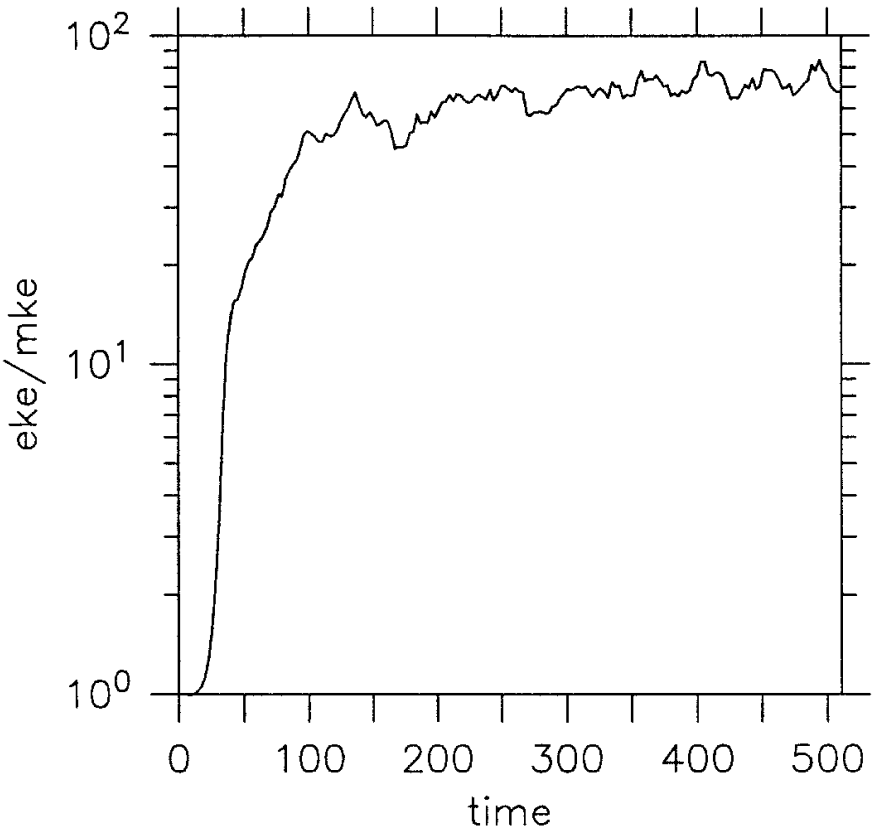

Figure 6. Ratio of eddy kinetic energy to mean kinetic energy of the linear wind-driven flow as a function of nondimensional time for a wind-driven subtropical gyre with $U/\beta L_d^2 = 1.5$, other parameters defined in the text. The eddy kinetic energy is approximately 75 times the mean kinetic energy at equilibration.

boundary. The wind stress curl for the subtropical gyre is specified as

$$W_i = \tau_m \sin(\pi y/L_y). \tag{10}$$

In an ocean basin with a solid western boundary, energy that propagates westward at large scales is reflected eastward at small scales, at which point it is presumably dissipated. The westernmost 450 km of the model domain contains an active sponge layer which restores the fields toward the linear, inviscid wind-driven solution. This combination of open boundary conditions together with damping toward the linear solution acts as a sink to large-scale, westward propagating energy and mimics the energy loss expected with a solid boundary. While this is not the physically most realistic western boundary condition, it has the conceptual advantage that strong western boundary currents are not supported so that all of the mesoscale energy generated in the model must derive from the large-scale wind-driven interior flow.

The time series of the ratio of total kinetic energy to initial kinetic energy for a typical wind-driven gyre case is shown in Figure 6. The eddy energy equilibrates at approximately 75 times the mean kinetic energy. The parameters for this model run are: $L_d = 25.8$ km, $\beta = 2 \times 10^{-11}$ m^{-1} s^{-1}, $U/\beta L_d^2 = 1.5$, $C_d = 0.0$. The basin is dimensioned 3000 km by 3000 km.

The early evolution of the initial small perturbations is much like what was found for the meridional channel calculations. Initially random perturbations develop into zonally elongated waves with meridional wavelength of $O(2\pi L_d)$ by time 30 (Fig. 7a). These wave packets are advected to the south by the mean flow and also drift to the west due to the beta-effect. Secondary instabilities grow on these zonal jets which give rise to an energetic mesoscale eddy field. There are also small perturbations that develop in the nearly zonal regions of the flow (i.e., near the northwest corner), yet these are unable to reach very large amplitude because of the influence of β, as discussed by Pedlosky (1975) and HL96. Although linear theory indicates that such zonal mean flows have a faster growth rate than meridional mean flows, the nonlinear theory developed in the preceeding section indicates that the slower growing meridional flows equilibrate at much higher eddy kinetic energy.

The rapid kinetic energy growth phase is characterized by the turbulent cascade of these eddies toward larger length scales, as found for the meridional channel flows considered in the previous section. The upper layer streamfunction at time 400 is shown in Figure 7b. The interior of the basin is now dominated by the mesoscale eddy field with length scales larger than the deformation radius and smaller than the basin-scale. The wind-driven flow is not evident in this synoptic view; however, the time mean fields reveal an anticyclonic large-scale circulation quite similar to the initial linear wind-driven flow.

A series of model calculations have been carried out in which the parameter $U/\beta L_d^2$ is varied (Fig. 8). In one case, the strength of the wind-driven flow was held fixed at $U = 1$ cm s^{-1} and L_d was varied between 10 km and 28.9 km (squares). In the other set of calculations, the internal deformation radius was held fixed at $L_d = 15.8$ km and the strength of the wind-driven flow was varied between 0.375 cm s^{-1} and 4 cm s^{-1} (triangles). The eddy kinetic energy varies between 25 and 300 times the mean kinetic energy. The increase in eddy energy with the model parameters agrees reasonably well with the scaling theory. These calculations emphasize the importance of the internal deformation radius in determining the eddy energy level. The range of $U/\beta L_d^2$ is similar in both sets of calculations, yet the cases where U is held fixed and L_d is varied produce a much wider range of eddy kinetic energy levels than is found when L_d is fixed and U is varied.

The direction of the mean flow in the wind-driven gyre is a function of the aspect ratio $\alpha = L_x/L_y$. When the aspect ratio is small the wind-driven flow is oriented in a nearly meridional direction over most of the basin. In the limit of very small aspect ratio the results are expected to approach the meridional channel case. As the aspect ratio increases the region of the flow that is nearly meridional decreases. Because the zonal potential vorticity gradient is supported by the meridional flow, the region of the domain with significant stores of potential energy that can be converted via zonal motions decreases with increasing aspect ratio. Thus, it is expected that the equilibration amplitude will depend on the aspect ratio of the basin.

A series of calculations have been carried out in which $L_d = 18.3$ km and $U/\beta L_d^2 = 1.5$ are held fixed and the basin size is varied. The equilibration amplitudes are plotted in Figure 9 for L_y of 3000 km (squares), 4500 km (triangles), or 6000 km (circles). The only

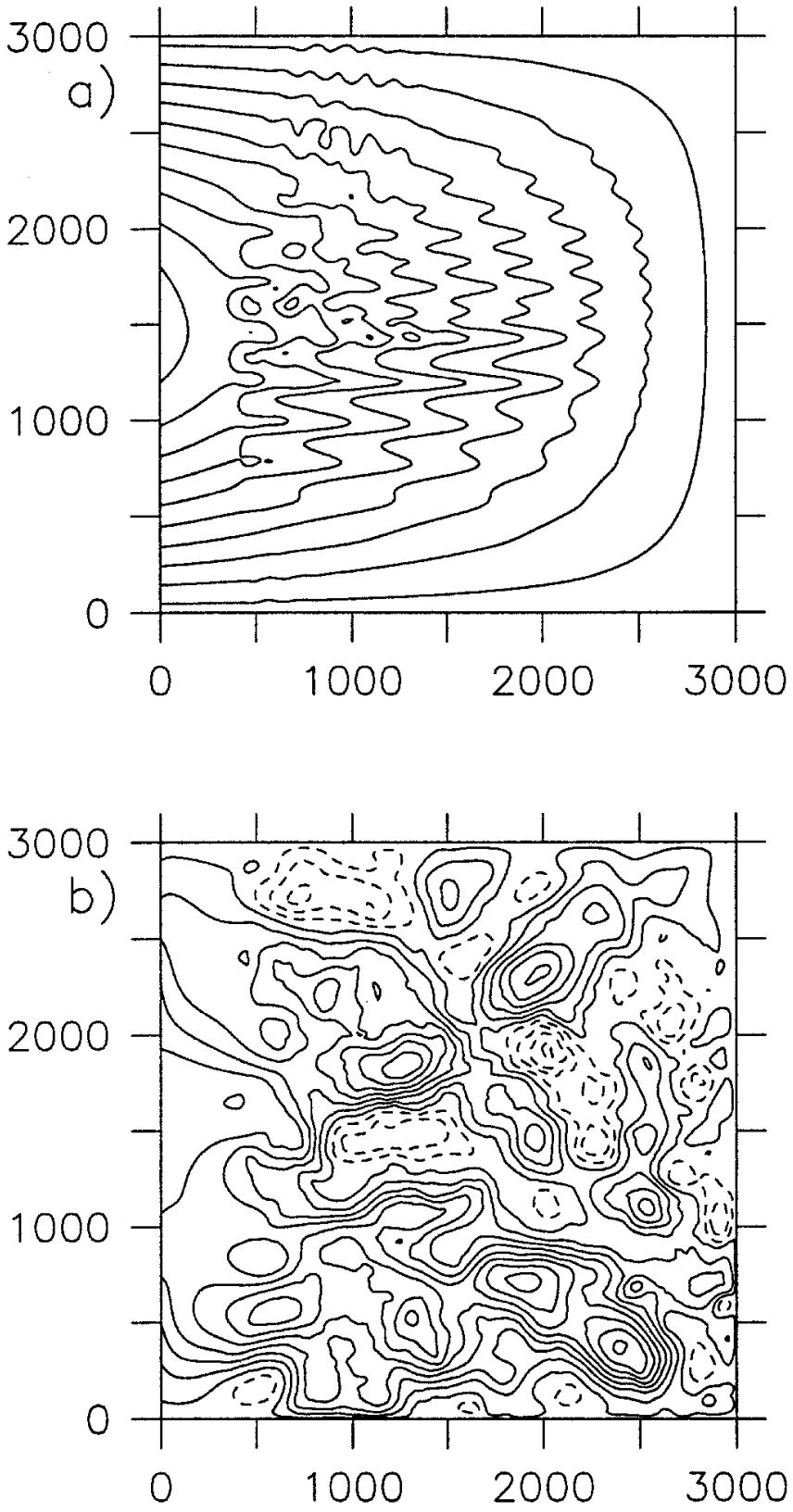

Figure 7. Layer 1 streamfunction for a subtropical at time (a) 30 (contour interval is 0.001) and (b) 400 (contour interval is 0.002). The early development of strong zonal jets and their subsequent instability is reminiscent of the meridional channel flows in Section 3a. The equilibrated phase is characterized by very strong, nearly homogeneous and barotropic eddies with length scales much larger than the deformation radius.

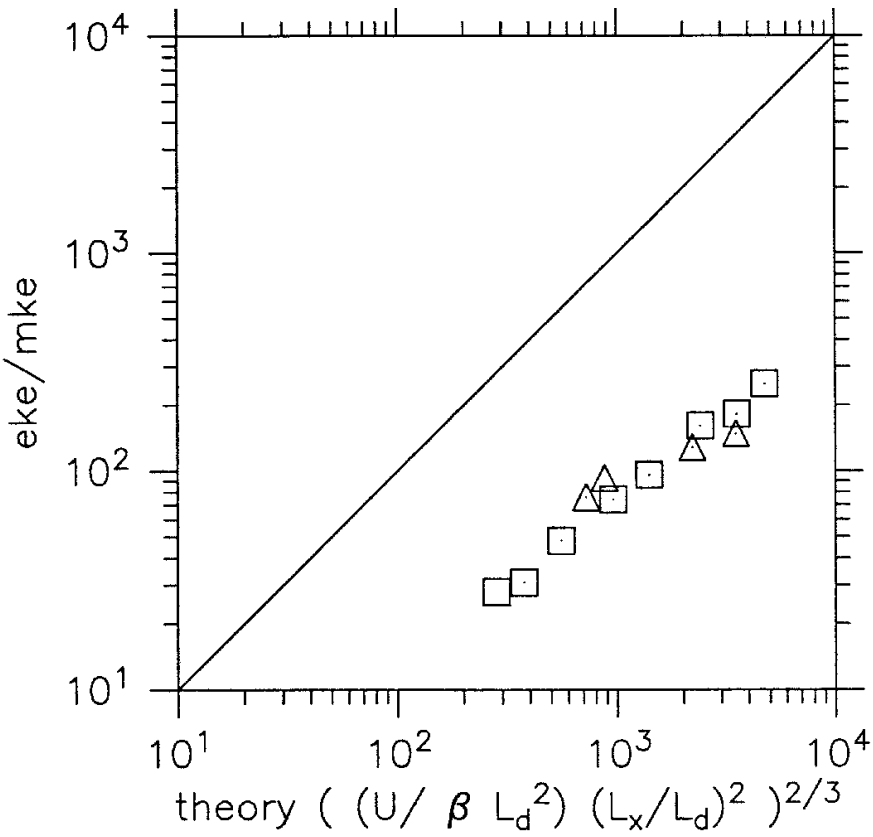

Figure 8. Comparison between the eddy kinetic energy (normalized by the mean wind-driven kinetic energy) found in the model at equilibration compared to that predicted by the scaling theory for the wind-driven subtropical gyre. The parameter $U/\beta L_d^2$ is varied between 0.6 and 5.0 with U = 1 cm s^{-1} km (squares) and between 1 and 8 with L_d = 15.8 km (triangles), other details of the calculations are given in the text. The eddy kinetic energy is between 25 and 300 times greater than the mean kinetic energy. The parameter dependence predicted by the scaling estimate (6) is reasonably well reproduced by the model.

difference between calculations at the same theoretical estimate for the eddy amplitude in Figure 9 is the meridional extent of the basin, or the aspect ratio. The model results are nearly independent of L_y, or aspect ratio, for $\alpha < 1$. As L_x increases until $\alpha > 1$ the eddy energy level becomes independent of further increases in L_x. This occurs at different energy levels depending on the meridional extent of the basin. The eddy amplitudes for the largest basin size (6000 km, circles) continue to increase in good agreement with the scaling theory for the largest zonal dimensions tested. It is worth noting that, even for those calculations in which the amplitude of the eddy kinetic energy is limited by the aspect ratio, the scaling theory correctly predicts the dependence of the eddy amplitude on the other model parameters (Fig. 8).

4. Summary

The objective of this study is to determine if weakly sheared meridional flows can generate strong mesoscale variability. Weak shear is defined here as $U/\beta L_d^2 = O(1)$, where U is the vertical shear of the mean flow, β is the meridional gradient of planetary vorticity,

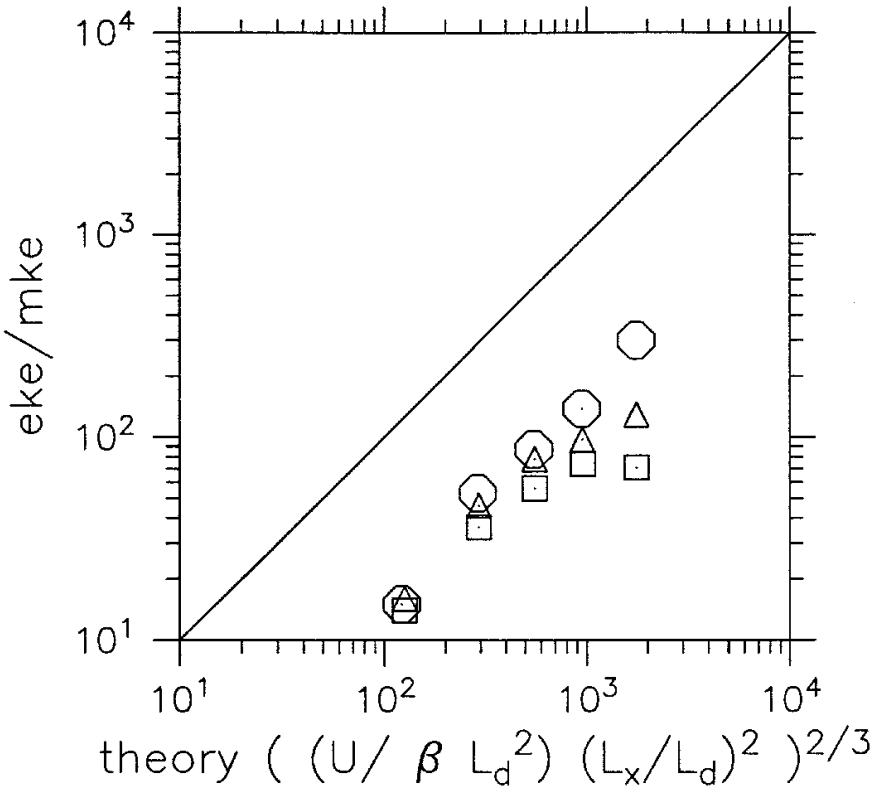

Figure 9. Eddy kinetic energy for the subtropical gyre for various basin configurations with $U/\beta L_d^2 = 1.5$ and $L_d = 18.3$ km. The meridional extent of the basin is 3000 km (squares), 4500 km (triangles) and 6000 km (circles). The zonal extent of the basin is varied between 550 km and 4050 km.

and L_d is the internal deformation radius. This issue is motivated by the observation that the eddy kinetic energy in the interior of the oceanic gyres is much larger than the mean kinetic energy. Baroclinic instability of the large-scale interior circulation was identified early on as a possible candidate, but subsequent nonlinear analysis indicated that for weakly sheared *zonal* mean flows, the eddy kinetic energy is approximately bounded by the mean kinetic energy (Pedlosky, 1975; HL96). The introduction of a nonzonal component to the mean flow removes this constraint by providing a source of potential energy that may be converted to kinetic energy by unstable waves without being inhibited by the planetary vorticity gradient. As a result, the zonal dimension of the basin (relative to the internal deformation radius) emerges as an important factor in determining the equilibration eddy amplitude.

There have been many recent attempts to parameterize the eddy flux of tracers as a function of the local properties of the mean flow (see Visbeck *et al.,* 1997 for a review). The meridional flow studied here is one example of a situation in which the amplitude of the eddy kinetic energy, and of the eddy flux of tracers, depends fundamentally on a nonlocal aspect of the flow, the zonal dimension of the basin. It is also evident that the direction of the mean flow is very important in determining the amplitude of the eddy flux of tracers, a property that has not been traditionally considered in eddy flux parameterization schemes.

Although the present results suggest that instability of weak meridional flows in the open

ocean may be an important eddy generation mechanism, it is still not clear whether the observed eddies are due to local instabilities, radiation from remote sources, or local forcing (such as by the wind). One apparent discrepancy between the eddies produced in these simple calculations and those in the ocean is in the length scale. Altimeter data indicate that the dominant length scale of the near-surface mesoscale eddy field scales with the baroclinic deformation radius (Stammer, 1997), while the present results produce larger, nearly barotropic eddies of the Rhines scale. However, recent theoretical and numerical results suggest that nonuniform stratification may inhibit the energy cascade towards large scales in both freely evolving flow (Smith and Vallis, 2000) and in forced/dissipative systems (Brian Arbic, private communication). Bottom topography may also limit the extent to which eddies can cascade to very large scales (Treguier and Hua, 1988; Brian Arbic, private communication). Nonetheless, the finding that nonzonal flows can generate large eddy kinetic energies should remain relevant even in the presence of more realistic stratification and bottom topography.

There are two major points resulting from this study.

1. Weakly sheared meridional flows can generate eddy kinetic energy that is two to three orders of magnitude greater than the mean kinetic energy for flow parameters typical of the mid-latitude subtropical gyres.

2. Scaling estimates of the eddy amplitude that are based on a balance of energy production through baroclinic eddy fluxes and energy cascade through two dimensional turbulence agree reasonably well with results from nonlinear model calculations.

Acknowledgments. Support for this work was provided by the National Science Foundation through the Atlantic Circulation and Climate Experiment under Grant OCE-95-31874. Natalia Beliakova is thanked for providing an early version of the numerical model used in this study. This work has benefited from many interesting conversations with Joseph Pedlosky. This is Woods Hole contribution number 10023.

REFERENCES

Beliakova, Natalia Y. 1998. Generation and maintenance of recirculations by Gulf Stream instabilities. Ph.D. thesis, Massachusetts Institute of Technology/Woods Hole Oceanographic Institution, 224 pp.

Crease, J. 1962. Velocity measurements in the deep water of the Western North Atlantic. J. Geophys. Res., *67,* 3173–3176.

Dubus, Laurent. 1999. Baroclinic instability of the NE Atlantic mid-latitude meridional currents. Impacts on the large scale circulation and associated tracer mixing. PhD thesis, Universit de Bretagne Occidentale, Brest, France.

Gill, A. E., J. S. A. Green and A. J. Simmons. 1974. Energy partition in the large-scale ocean circulation and the production of mid-ocean eddies. Deep-Sea Res., *21,* 499–528.

Held, Issac M. and Vitaly D. Larichev. 1996. A scaling theory for horizontally homogeneous baroclinically unstable flow on a beta-plane. J. Atmos. Sci., *53,* 946–952.

Larichev, Vitaly D. and Issac M. Held. 1995. Eddy amplitudes and fluxes in a homogeneous model of fully developed baroclinic instability. J. Phys. Oceanogr., *25,* 2285–2297.

Panetta, R. Lee. 1993. Zonal jets in wide baroclinically unstable regions: Persistence and scale selection. J. Atmos. Sci., *50,* 2073–2106.

Pedlosky, J. 1975. A note on the amplitude of baroclinic waves in the mid-ocean. Deep-Sea Res., *22,* 575–576.

—— 1987. Geophysical Fluid Dynamics, Springer-Verlag, NY, 624 pp.

Rhines, Peter B. 1975. Waves and turbulence on a beta-plane. J. Fluid Mech., *69,* 417–443.

—— 1977. The dynamics of unsteady currents, *in* The Sea, Vol. 6, E. A. Goldberg, I. N. McCave, J. J. O'Brien and J. H. Steele, eds., Wiley, 189–318.

Robinson, A. R. 1983. Eddies in Marine Science, Springer-Verlag, 609 pp.

Robinson, A. R. and J. C. McWilliams. 1974. The baroclinic instability of the open ocean. J. Phys. Oceanogr., *4,* 281–294.

Salmon, R. 1980. Baroclinic instability and geostrophic turbulence. Geophys. Astrophys. Fluid Dyn., *15,* 167–211.

Smith, K. S. and G. K. Vallis. 2000. The scales and equilibration of mesoscale ocean eddies. Part I: Freely evolving flow. J. Phys. Oceanogr., (submitted).

Spall, M. A. 1999. A simple model of the large-scale circulation of Mediterranean Water and Labrador Sea Water. Deep-Sea Res. II, *46,* 181–204.

—— 1994. Mechanism for low-frequency variability and salt flux in the Mediterranean salt tongue. J. Geophys. Res., *99,* 10,121–10,129.

Stammer, D. 1997. Global characteristics of ocean variability estimated from regional TOPEX/ Poseidon altimeter measurements. J. Phys. Oceanogr., *27,* 1743–1769.

Swallow, J. C. 1971. The Aries current measurements in the Western North Atlantic. Philosophical Transactions of the Royal Society, *270,* 451–460.

Treguier, A. M. and B. L. Hua. 1988. Influence of bottom topography on stratified quasi-geostrophic turbulence in the ocean. Geophys. Astrophys. Fluid Dyn., *43,* 265–305.

Visbeck, M., J. Marshall, T. Haine and M. Spall. 1997. Specification of eddy transfer coefficients in coarse-resolution ocean circulation models. J. Phys. Oceanogr., *27,* 381–402.

Received: *7 September, 1999;* revised: *16 December, 1999.*